Reducing societal impacts of SARS-CoV-2 interventions through subnational implementation

Mark M. Dekker[1,2,3 †], Luc E. Coffeng[4], Frank P. Pijpers[5,6], Debabrata Panja[1,2 *], and Sake J. de Vlas[4 *]

[1]Department of Information and Computing Sciences, Utrecht University, Utrecht, The Netherlands
[2]Centre for Complex Systems Studies, Utrecht University, Utrecht, The Netherlands
[3]PBL Netherlands Environmental Assessment Agency, The Hague, The Netherlands
[4]Department of Public Health, Erasmus MC, University Medical Center Rotterdam, Rotterdam, The Netherlands
[5]Statistics Netherlands, The Hague, Netherlands
[6]Korteweg-de Vries Institute for Mathematics, University of Amsterdam, Amsterdam, Netherlands
[†]m.m.dekker@uu.nl
[*]Senior authors contributed equally

March 31, 2022

Abstract

To curb the initial spread of SARS-CoV-2, many countries relied on nation-wide implementation of non-pharmaceutical interventions, at a high socio-economic cost. Using the first COVID-19 wave in the Netherlands as a case in point, we address how subnational implementations might have achieved similar levels of epidemiological control with fewer societal consequences; e.g., parts of the country could have stayed open for longer. To this end, we develop a high-resolution analysis framework reflecting a demographically stratified population with a spatially explicit, dynamic, individual contact pattern-based epidemiology, exploiting mobility trends extracted from mobile phone signals and Google mobility. The framework is exportable to other countries and settings, and may be used to develop policies on subnational approach as a better strategic choice for controlling future epidemics.

Introduction

As in many countries around the world [1, 2], control of the first COVID-19 pandemic wave in the Netherlands was largely based on nation-wide implementation of a variety of non-pharmaceutical intervention measures (e.g., lockdown, social distancing, or reduced mobility). Their associated societal burden affected all areas in the country equally, while infections and the healthcare burden, in contrast, were distributed heterogeneously across space and time. This brings in focus the question whether the pandemic could have been controlled equally well with interventions specifically tailored to subnational regions, such as municipalities or provinces. In addition to preventing the unnecessary broader societal burden of interventions in (largely unaffected) parts of a country, such tailored strategies potentially have several additional advantages: (1) more efficient use of resources, such as test kits and mobile laboratories; (2) reduced economic losses due to interventions; (3) reducing intervention-adherence fatigue in the population.

Epidemiological analyses can help to explore the value of such strategies [3]. However, the challenge therein lies in the fact that epidemiological dynamics cannot easily be untangled from human behavior, which varies strongly across societies and cultures [3], and are highly heterogeneous even within a population living in a certain geographic region [4, 5]. For this reason, such an epidemiological analysis not only needs to capture the spatio-temporal heterogeneities in both transmission and control of an infectious disease, but also "to embed itself locally" [6, 7]: the demographic composition of the population and how people travel, interact and mingle, across different demographic groups and subnational regions [8–10]. Building a corresponding analysis framework that takes all this into account is however not only highly complex, but also requires rich data at high resolutions.

Such challenges have left their vivid marks in the first COVID-19 wave. By and large, intervention measures deployed in spring 2020 were not enough to spatially contain the virus: the worldwide spread of SARS-CoV-2 along the backbones of globalized travel was too fast to allow continuation of travel as usual. Reliable data (specifically, near real-time data needed for policy-informing epidemiology) on community-transmission were not readily available to researchers and policy makers during most part

of the first wave. For setting intervention policies in such a situation, large parts of the world used epidemiological insights that were emerging from other countries that experienced the epidemic earlier, notably China [11, 12]. First, this meant that local embedding was being missed [7]. Second, by the time reliable data started to become available, national policies in many countries, e.g., the Netherlands [13] or the UK [14], were mostly informed by models considering populations that were demographically but not spatially heterogeneous [15].

Here, using the Netherlands as a case in point, and supported by a combination of rich data sources (demography, mobility, mixing, hospitalization and seroprevalence), we develop an epidemiological analysis of the first COVID-19 wave by building a dynamic proxy network of people's contacts to embed into the local context as well as to account for high-resolution spatio-temporal heterogeneities [16]. The wave covers the period February 27, 2020 (the first tested case of COVID-19 in the Netherlands) till June 1, 2020 (lifting of most intervention measures). In this timeline, there are four distinguishable periods in terms of the policy landscape, which we refer to as *phases*: (i) Phase 1 (Feb 27 - Mar 11) when transmission of the pathogen progressed unchecked, (ii) Phase 2 (Mar 12 - Mar 22) with minor interventions involving a working-from-home policy, cancellation of large events, some social distancing and face mask advice in specific buildings such as hospitals, (iii) Phase 3 (Mar 23 - May 11) involving a strict nation-wide lockdown with closed schools and event centers, mandated social distancing and working-from-home policies, and (iv) Phase 4 (May 11 - May 31) involving a gradual lifting of all measures. The analysis not only allows us to individually assess the efficacy of the (national) non-pharmaceutical intervention measures that were implemented in the Netherlands, but it also allows us to investigate to what extent subnational implementation of interventions during the first wave of COVID-19 would have led to poorer or comparable control of the pandemic in the country as a whole. In larger countries the most appropriate subnational resolution could be at the level of counties, provinces, or any other existing administrative regions to make best use of clear lines of communication and responsibilities; in a small, densely populated country like the Netherlands, municipalities are the most appropriate ones. Our analysis can be exported to any other country provided comparably rich datasets, capturing the local embedding for the analysis, are available.

Analysis framework

Taking an agent-based approach, we build our framework in two parts: (i) demography, mobility and mixing considerations that provide a high-degree of local embedding, and (ii) transmission and interventions, each consisting of four steps (1-4 and 5-8, respectively in Fig. 1). The key steps for the epidemiological dynamics are summarized below; additional details can be found in the methods section and SI A.1-A.8 (one SI A section per step).

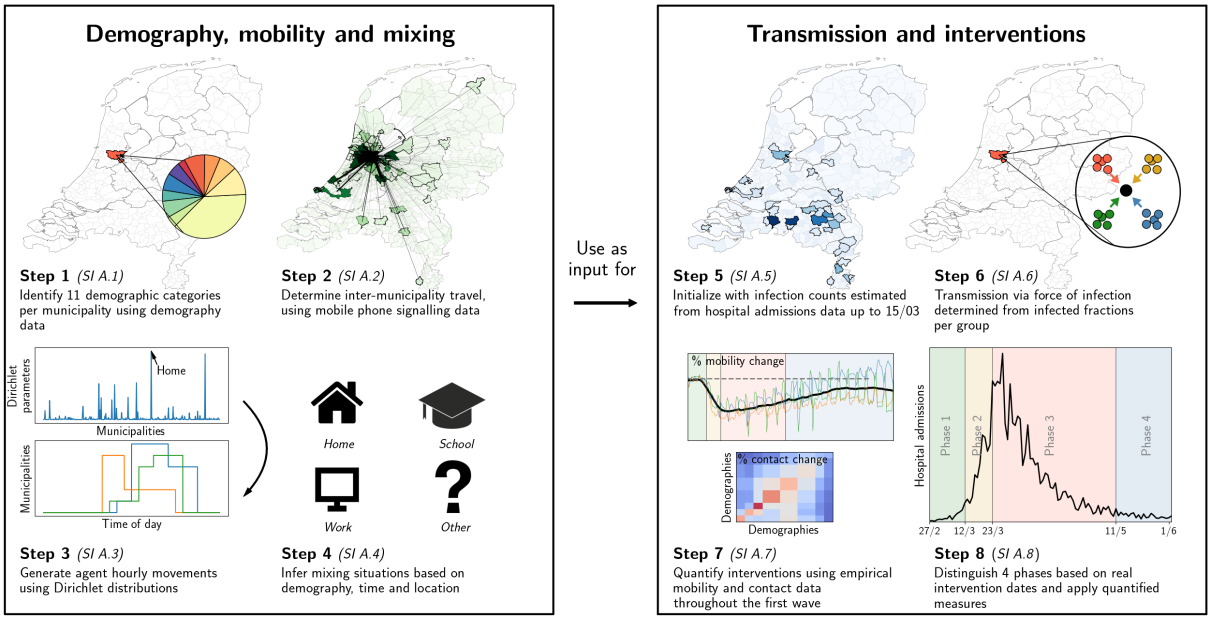

Figure 1: Our analysis framework consists of two parts: establishing proxy dynamic contact patterns from information on demography, mobility and mixing (left panel), and transmission and interventions (right panel); each part consists of four further steps. See SI B.1 for a detailed description of the data used in steps 2 and 5. Processes in steps 2, 3 and 6 are stochastic in nature.

In the first part, we define the agents and their movements. In the first step, using registry data available at the Dutch national statistics agency (CBS, Statistics Netherlands), we stratify the Dutch population into 11 demographic categories and 380 municipalities. With about 17 million Dutch residents, we define an *agent* to represent approximately 100 Dutch residents. We distribute the agents across municipalities proportionally to population sizes. The second step is to define the probability that an agent moves between municipalities. This process is constructed using Dirichlet distributions for the probability of an agent's location, quantified based on anonymized mobile phone signals. In the third step, we draw the agent's locations and movements at hourly time resolution. The fourth step is to define the mixing of agents present within the same municipality, which depends on the demographic category of the agent, time of day and the type of activity that the agent is engaged in: 'home' , 'school', 'work' and 'other'. The corresponding mixing matrices were based on existing surveys [9]. Together, the four steps establish a dynamic proxy network of people's contacts throughout the entire country at municipality-level, with hourly resolution over the full period of analysis.

The second part of the analysis covers transmission and interventions. Here, the fifth step concerns the initialization of the epidemic transmission model, which was based on observed hospital admissions, which initially occurred mainly in the south of the country. The sixth step was to define transmission, based on the SEIR model for agent-to-agent pathogen transmission, which means that every agent at any time has one of the following four labels: susceptible (S), exposed (E), infected (I) and recovered (R). Every one-hour time step, susceptible agents may move to the exposed compartment as a result of the *force of infection* that they experience as a function of the prevalence of infectious cases in each demographic category in the same municipality, expected contact rates between the agent and the different demographic categories, and their respective infectiousness. The seventh step concerns the quantification of changes across the first COVID-19 wave: (i) behavioral measures that reduce contact rates, (ii) mobility reductions, and (iii) school closure. Mobility changes were computed using Google Mobility data and mixing changes were based on survey data [17] conducted during this period. The effect of behavioral measures were calibrated to reproduce the epidemic trend over time. In the final step, we simulate transmission and the effect of changes in interventions over time. Predicted trends in infection numbers were translated to incident and prevalent hospital admission using a simple cohort model [18] that accounts for the delay between initial infection and admission as well as the duration of admission. This cohort model was quantified based on hospitalization data from the Dutch National Intensive Care Evaluation (NICE) registration.

A summary of the analysis itself can be found in the Methods section.

Reproducing the first COVID-19 wave

Even for a geographically heterogeneous analysis it is necessary to verify that the national trends are reproduced, which serves to calibrate and validate the relevant parameters in our simulations. The results of the calibration process, carried out by means of an ensemble of 40 stochastic simulations, is shown Fig. 2(a-b). The calibration is performed by means of four transmission-related parameters — β_1 through β_4, one for each phase of the first wave — to reproduce the *total national* hospital admissions data spanning approximately three months [panel (a)], including the (initial) doubling time [panel (b)]. Hospital admissions were the most reliable source of data during the first wave, and are shown in Fig. 2 as a thick black line in both panels, with the red line and its margins showing the range produced by our simulations. The curves in other colors in panel (a) denote the numbers of infected and exposed people, obtained from simulations. See Methods for the β_t-parameter values, and SI A.8 for the details of the calibration process.

Age stratification in our analysis reveals how the first wave likely played out nationally across demographic groups, with non-studying adolescents, middle-age working people, and students as the most affected demographic groups [Fig. 2(c)]. The model predicts similar patterns for seroprevalence levels across age as was observed in June 2020 [Fig. SI B.2]. It also predicts that the epidemic geographically spread from the south (where COVID-19 is introduced in the analysis) to the north of the country via major cities in the west [Fig. 2(d)]. This geographic pattern approximately reflects the actual spread in the Netherlands, although we should not expect the analysis to perfectly reproduce given the high variability in the ensemble runs (see SI B.4). Finally, in panel 2(e) the hospitalization data over time are compared for three different locations in the Netherlands: the first Dutch outbreak site in the South (Eindhoven), a location in the West (The Hague) where the epidemic spread relatively quickly, and a site in the North (Groningen) which was affected less and also later. That only four (national-level β_t-) parameters leads to realistic geographical spread across 380 individual municipalities over time serves to validate our approach for a geographically heterogeneous analysis (next section).

After the satisfactory calibration process above, we use the analysis to unravel the impact of individual

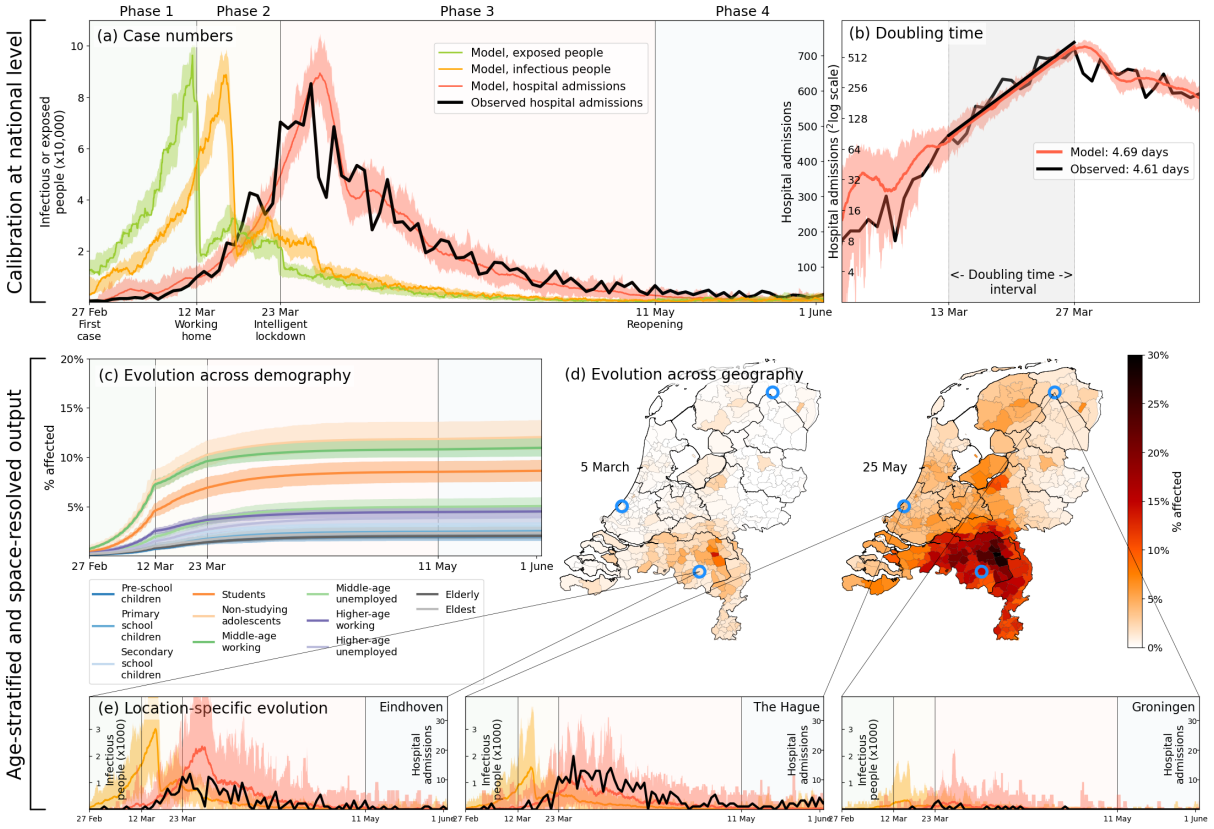

Figure 2: Calibration (a-b), and demography- and geography-resolved results from our analysis (c-e). **Panel (a)**, left axis: the daily number of new infections and exposures in yellow and green, respectively. Right axis: daily hospital admissions from analysis output (red) and observed data (black). Background colors and vertical black lines denote the four phases (arbitrary coloring). Uncertainty intervals mark the minima and the maxima in the ensemble of realizations used in the analysis; the same holds for panels (b), (c) and (e). **Panel (b)**: Hospitalization doubling time over the period March 13 - March 27, 2020 (shaded gray shaded time domain) in analysis (red, 4.69 days) and observed data (black, 4.61 days). **Panel (c)**: % affected agents (i.e., E, I or R) per demographic group over time. **Panel (d)**: % affected agents per municipality on two days (March 5, May 25). Blue circles indicate the geographical locations of the three example municipalities shown in panel (e). **Panel (e)**: Infected agents (yellow) and hospital-admitted agents (analysis in red, and observed data in black) in three municipalities in different municipalities: Eindhoven, The Hague and Groningen. Analysis data correspond to an ensemble of 10 independent realizations.

lockdown components (behavior, mobility, school closure). Figure 3(a), again a 40-member strong ensemble, shows how reductions in mobility contributed most to epidemic control; without mobility restrictions (red), case numbers would have approximately doubled. Behavioral changes (blue) have also had a considerable impact, albeit lower than mobility. (Determining the impact of the behavioral intervention measures is fairly straightforward: rather than varying the values of the transmission-related parameters β_1-β_4, we simply keep all at the same value as for the very first phase.) Our analysis also predicts school closure [yellow, Fig. 3(a)] to have had little impact. On this, we note that due to political debate, the Dutch schools were closed relatively late (March 16, while the first confirmed case was on Feb 27) and therefore have contributed little to epidemic control in our analysis (logically, earlier closure of schools should have had a positive epidemiological impact, see SI B.3). The individual lockdown components contributed similarly to spatial spread [Fig. 3(b)], which quantifies the geographic spread of the COVID-19 pandemic in the Netherlands by following the number of municipalities affected substantially (for this, we use the measure of having $> 0.08\%$ of population hospital admitted).

Effects of subnational implementation of interventions

Next, we evaluate the potential of subnational interventions, which in the Dutch case concerns non-pharmaceutical interventions issued at the level of municipalities. For a fair comparison across scenarios and with hospital admission data during the first wave, we implement subnational interventions in our simulations following the national trend. This means that we initiate lockdown in a municipality when the simulated prevalence of infectious cases within that municipality has passed a certain threshold — a fraction of the municipality's population — where the exact intervention measures are synchronous those issued in reality on a national scale (SI A.9). Choosing the value of this threshold poses a trade-off: a lower threshold ensures implementation of local interventions in an early stage of the COVID-19 wave

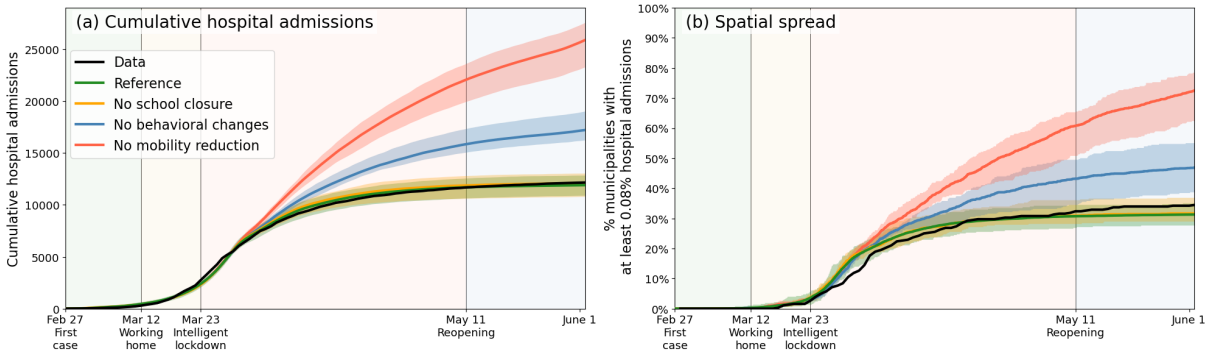

Figure 3: Comparing the impacts of nationally administered intervention measures. In both panels, observed data are shown in black, the reference in green, and the impacts of (i) no behavioral changes like wearing masks, enhanced hygiene and social distancing in blue, (ii) no mobility reduction in red and (iii) no closing of schools in yellow. Bandwidths indicate the minima and maxima around the mean of a simulation ensemble of 40 realizations. **Panel (a)**: Cumulative national hospital admissions. **Panel (b)**: Geographical spread of hospital admissions, measured by the fraction of municipalities that have at least 0.08% of the population admitted to the hospital.

which would suppress hospital admission counts, but could unnecessarily shut down economic and social activity in some parts of the country that are less affected by the disease. Vice versa, a higher threshold would target municipalities where the epidemic has progressed most, but could pose the risk of starting control too late, resulting in more hospital admissions. To show the effect of different thresholds for prevalence of infectious cases, we choose a wide range of 3%, 1%, 0.33% and 0.1%. Our choice to use prevalence of infectious cases for local decision-making is motivated by the following premise. Even though testing and case reporting were not yet at a sufficient scale to inform local decisions during the first wave, since then they were significantly scaled up. Moreover, with emerging methods and technologies such as sewage monitoring, fast identification of disease biology (e.g., time until symptoms) and live tracking of infections by mass testing [19] and using apps, number of infections in future will be proxy-estimated with progressively greater accuracy and speed, facilitating faster decision-making on subnational intervention measures (such as, in the Netherlands, starting or scaling down lockdowns at the level of municipalities).

The results are shown in Fig. 4. In panel (a), the epidemiological impact of subnational interventions is quantified in terms of the number of hospital admissions, while the societal impact is quantified in panel (b) by the number of municipalities that are undergoing interventions. In panel (a), the lockdown as implemented in the Netherlands is represented by the black (observed) and green lines (prediction), which resulted in approximately 13 thousand hospital admissions up to 1 June 2020. Higher thresholds for deciding to implement a local lockdown clearly result in higher numbers of cumulative hospital admissions [panel (a)] and correspondingly a lower number of municipalities affected [panel (b)], and vice versa. A decision-making threshold of 3% (dark red) can be seen to be too high; although it allowed for 185 million additional person-days spent without interventions, it results in a 157% increase in number of admissions ($\sim$ 19 thousand). The more stringent thresholds of 1.0% and 0.33% result in numbers of hospital admissions closer to a national lockdown (4,670 and 355 additional admissions, respectively), but at a more modest societal benefit (103 million and 36 million additional person-days free from interventions, respectively). Interestingly, at the lower threshold of 0.33% (yellow), approximately 6% of the municipalities could remain without interventions for the full duration of the first wave. The maps [Fig. 4(c-d)] show the corresponding geographical distribution of percentages of affected people, i.e., people who would have been hospitalized [panel (c)] and the societal benefits of subnational interventions in terms of the fraction of simulation-ensemble realizations in which a municipality remains without interventions [panel (d)]. Municipalities that remain free of interventions are mainly located in the north and east of the country, as can be most clearly seen for the 0.33% threshold scenario. From a mobility perspective, these municipalities belong to the more rural, isolated, and less densely populated subnational regions of the country.

During the first COVID-19 wave, the Dutch government did not implement subnational intervention measures, aside from bringing out an early advice to work from home in the south of the country, the epicenter for the first wave. The reasoning was that once COVID-19 cases were discovered locally, most likely, the pathogen would have already spread throughout the entire country. This is generally in line with observations that the Netherlands is spatially well-connected in terms of people's mobility patterns, facilitated by a robust public transport system and a high population density, with the caveat that hospital admission data during the first wave did suggest that provinces in the north and east of the country were substantially less affected. Our results show that when combined with live tracking of local infections in sufficient detail, implementation of interventions could be postponed or tailored towards local contexts,

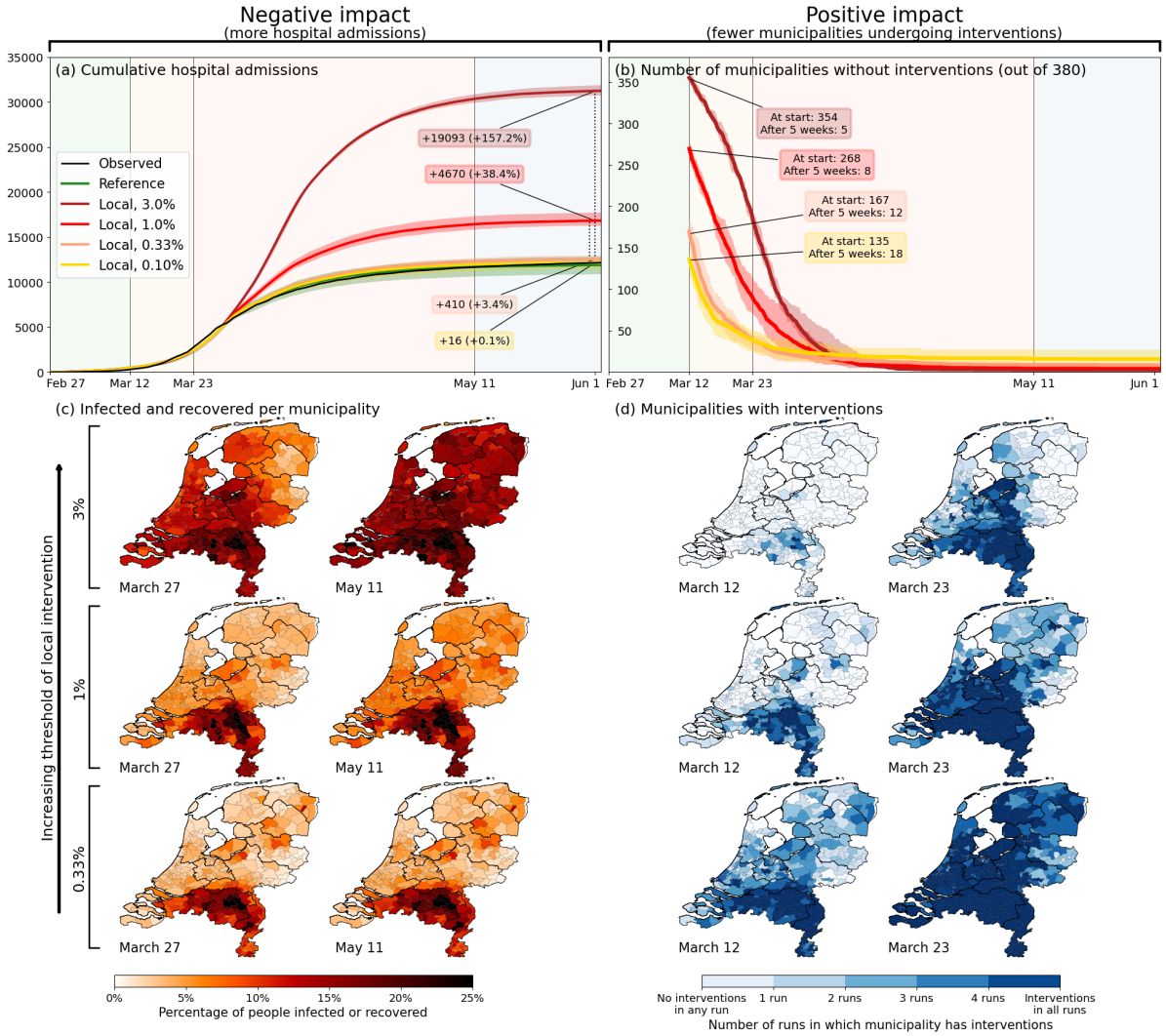

Figure 4: Quantification of the trade-off between costs (left) and benefits (right) of locally-adjusted interventions at four threshold values (0.1%, 0.33%, 1% and 3% of population simultaneously infected). **Panel (a)**: Cumulative hospital admissions for different scenarios. **Panel (b)**: Fraction of municipalities that do not have any interventions in place. **Panel (c)**: Cumulative fraction of infection cases per municipality for the three local intervention thresholds. The additional number and percentage growth in hospital admissions as compared to the observed national interventions is indicated. **Panel (d)**: Geographical indication of which municipalities have undergone interventions and which ones not. The number of municipalities that do not is shown in panel (b).

without causing too much additional health burden. (This would of course require local governments to be mandated appropriately and that local populations adhere to local measures.)

Discussion and conclusion

Using the Netherlands as a case in point, we have evaluated the contribution of different interventions to the total effect of the lockdown, and explored to what extent subnational implementations of intervention measures might have had less of a societal impact, but comparable epidemiological impact. To this end, we have developed a highly detailed geographically- and demographically-stratified analysis framework based on a dynamic proxy network of people's contacts throughout the entire country at municipality-level, with hourly resolution, which in turn utilizes human mobility between municipalities based on mobile phone signal data. We found that in the Netherlands mobility reductions during the first wave contributed most to epidemic control; without, a doubling of hospital admissions was predicted to have occurred. Our analysis, albeit based on a small country, shows that subnational (translated to be at the municipality-level) implementation of interventions strategies is worth considering, provided that means to monitor infection levels are available (via sewage surveillance [20], can substantially reduce the societal burden of interventions. The benefits of such an approach are expected to be even greater for larger and more populated countries. Moreover, similar or even higher gains can be expected by considering a subnational approach for also lifting interventions at a subnational level: analogous to initializing interventions, the reduction of the disease's prevalence across municipalities is not synchronous and, depending on the chosen

prevalence threshold, some will be able to lift earlier than was done nationally.

Even though the methodology proposed in this paper comprises demographic and geographic stratification, and distinguishes multiple circumstances of mixing, there are still forms of granularity that we omit (e.g., households), which limits our ability to evaluate the impact of specific interventions with higher precision [21]. For instance, when incorporating the effect of school closures, the effect of interacting only with family members instead of school mates has been captured at the level of a municipality as a whole (i.e., a different mixing pattern between demographic groups combined with an overall lower transmission rate). As such, our framework cannot provide insights into the role of households and household-level interventions, which have for instance been shown to play a critical role in the geographical spread of infection between schools [22, 23]. Another limitation is that mobility in our framework is quantified based on mobile phone signal data that only provide anonymized movements between pairs of locations. As such, the data do not provide identifiers to link multiple movements into one itinerary, which means that in our analysis, agent movements are somewhat shorter on average than in reality, but agents also visit more different locations than in reality. We further assume that agent movements vary randomly day-by-day, whereas in reality commuting means that an agent would repeatedly travel to the same location. However, the impact of this simplifying assumption is limited as, at the start of an epidemic, the distribution of movement over agents is of relatively low importance, especially in the case of a relatively small and highly connected country as the Netherlands. This is in contrast to situations towards the tail of an epidemic or in larger geographies (e.g., Brazil [24, 25] and India [26]), where the transmission potential of "high-mobility corridors" can eventually dry up as a result of rising immunity among high-mobility individuals. Finally, we adopted data on national patterns in mobility (Google mobility), meaning that it was not possible to account for changes in mobility by geography or demographic group. The geographical aspects could be addressed by using longitudinal mobile phone signal data or individual-level self-reported data via mobile phone apps [27–29]. This would require that such data are stored in a useful and accessible format in a General Data Protection Regulation (GDPR)–compliant manner, which may be challenging indeed.

In this study, we investigated only one of the several potential uses of our framework in a specific country. With appropriate data sources, the framework can be adapted to other countries and settings of similar or larger geographical scale. Importantly, the framework can also address other policy questions that involve a geographical or social dimension. For instance, we explored the potential impact of specifically isolating affected subnational areas (i.e., banning all mobility into and out of a municipality for the Netherlands), which could reduce hospital admissions by about 30%, compared to the actual national lockdown (SI B.3). With further expansions, the framework could address questions related to, for instance, closing or limiting specific (public) transport routes [30] and banning specific mass events [31–33] — for both of which much more fine-grained (temporal and geographical) data would be required. Evaluating pharmaceutical interventions such as vaccination, too, is possible to capture within this framework, upon coupling data sources associated with age-stratified vaccination rollout, as well as types of vaccines used.

In conclusion, we have shown that the potential added value of subnational implementation of interventions which, with appropriate information about infection levels in subnational areas, may significantly reduce the societal burden of lockdowns to control infectious disease. The main merit of our approach lies in the fact that it captures the local context by coupling empirical data sources on demography, mobility, and spatial clustering of the population and link this to disease transmission, which makes the approach exportable to other settings.

Methods

This section is devoted to discuss a few of the core concepts of the methods. For a detailed step-by-step explanation, see SI A.1-A.8.

Agents and their mobility patterns

The basis for the mobility patterns is anonymized mobile phone signal data gathered by a commercial dataprovider, resulting in numbers of daily travels by people living in municipality i to municipality j, split into frequent, regular and incidental movements. Additionally, the demographic data provided by Statistics Netherlands (CBS) allowed us to distinguish 170,721 agents (with roughly 17 million residents, this means that each agent represents about 100 of them) with demographic details (SI A.1). For each agent, we determine movements by drawing from mobility distributions computed from the mobile phone signal data, in which we distinguish frequent from incidental and regular movements by making assumptions about the reasons of moving (work and school versus other activity). More specifically, the generated mobility distributions are Dirichlet distributions, using the (normalized) movements data as shape parameters.

From these distributions, we independently draw fractions of the day spent in each municipality (i.e., resulting in 380 fractions for each of the 380 municipalities), that are subsequently converted into integer hours spent in municipalities. More detailed information on the computing of the agents' movements can be found in SI A.2 and SI A.3.

Pathogen transmission

Transmission from susceptible (S) to exposed (E) in this stochastic SEIR-based model is based on a "force of infection" λ, which is translated to an hourly infection probability. The idea behind λ exerted on a susceptible agent is that each demographic category contributes to the chance of transmission of the pathogen to this agent, weighted by the expected mixing between the agent and this category, as well as on the fraction infected in this category. The full equation for λ for people from demographic group g in municipality m at time t, involving a summation over all demographic groups g' adding to the force of infection, is as follows.

$$\lambda(g,m,t) = \underbrace{h(g)}_{\text{Susceptibility of } g} \cdot \underbrace{\beta_t \cdot \bar{s}(t)}_{\text{Phase \& daily cycle}} \cdot \underbrace{\sum_{\text{Group } g'} n_{g,g'} \cdot \frac{I(g',m,t)}{N(g',m,t)}}_{\text{Mixing with groups } g'}. \quad (1)$$

The first part on the right hand side of the equation involves a parameter $h(g)$ that reflects the susceptibility of an agent belonging to demographic group g to the disease (see SI A.1). The second part ($\beta_t \cdot \bar{s}(t)$) contains the behavioral parameter β_t (such as wearing face masks and maintaining social distance) depending on the phase of the wave (leading to β_1-β_4, see Table 1) and a daily cycle parameter $\bar{s}(t)$ (see SI A.6); e.g., ensuring that agents barely have any contacts in the middle of the night. The third part involves the mixing with the eleven different demographic groups: $n_{g,g'}$ is the expected number of contacts that group g has with group g', based on the mixing matrix that reflects the situation (i.e., 'home', 'school', 'work' or 'other'). The fraction $\frac{I(g',m,t)}{N(g',m,t)}$ is the fraction of the total number (N) of agents belonging to group g' in municipality m that are infectious (I).

The time scales of transitions from exposed (E) to infected (I) and from infected (I) to recovered (R) – expressed in an incubation and an infection time scale, respectively – differ per case and are drawn from Weibull distributions with mean time scales of 4.6 and 5 days, respectively [18] (SI A.5).

Phase	Start	End	Travel	Mixing	Behavior	Schools
1	Feb 27	Mar 11	-	-	$\beta_1 = 0.135$	Open
2	Mar 12	Mar 22	-31.7%	Reduced as per Apr 2020	$\beta_2 = 0.11$	**Closed halfway***
3	Mar 23	May 10	-42.4%	Reduced as per Apr 2020	$\beta_3 = 0.09$	**Closed***
4	May 11	Jun 1	-20.1%	Reduced as per Jun 2020	$\beta_4 = 0.11$	Open

Table 1: Overview of how the four phases in the first wave of COVID-19 in the Netherlands are implemented in our analysis. *Schools were closed in the period March 16 – May 10, which is also what we use in our analysis.

National-level interventions

The first COVID-19 wave in the Netherlands lasted over the period February 27 (first reported case) to June 1, 2020. Based on the interventions that took place, we split this period into four phases, for which we analyze the epidemiological impacts of changes in mobility, mixing, behavior and school closure. Details about these phases are shown in Table 1.

In our analysis, we capture these changes in the following manner. First, we reduce inter-municipality mobility as reported by Google [34] in the four phases of the first wave in the Netherlands. The dominant contribution to this travel reduction, by far, was due to a working-from-home policy recommended by the Dutch government; we implement it in our analysis by placing the reported percentage of agents, randomly drawn from the working categories, at home. Secondly, we address changes in mixing patterns by determining percentage changes in the mixing among different age groups from Dutch survey data [17] in the months February, April and June 2020, and applying these changes element-wise to the mixing matrices used in our analysis. Thirdly, we represent behavioral changes by variations in β_t in Eq. (1) across the four phases of the first wave. Fourth and finally, we implement school closing by placing school-going agents (i.e., primary school children, secondary school children and students) as well as the parents of primary school children at home, both in terms of the home locations of the agents and in terms of its implications on mixing (see SI A.7).

References

[1] J. M. Brauner, *et al.*, *Science* **371**, eabd9338 (2021).
[2] Y. Liu, *et al.*, *BMC Medicine* **19**, 40 (2021).
[3] P. G. T. Walker, *et al.*, *Science* **369**, 413 (2020).
[4] M. Marks, *et al.*, *The Lancet Infectious Diseases* **21**, 629 (2021).
[5] N. G. Davies, *et al.*, *Nature Medicine* **26**, 1205 (2020).
[6] E. R. A. Vos, *et al.*, *Journal of Epidemiology & Community Health* **75**, 489 (2021).
[7] R. M. Eggo, J. Dawa, A. J. Kucharski, Z. M. Cucunuba, *Nature Computational Science* **1**, 6 (2021).
[8] J. O. Lloyd-Smith, S. J. Schreiber, P. E. Kopp, W. M. Getz, *Nature* **438**, 355 (2005).
[9] K. Prem, A. R. Cook, M. Jit, *PLoS Computational Biology* **13**, e1005697 (2017).
[10] J. Mossong, *et al.*, *PLOS Medicine* **5**, 1 (2008).
[11] Q. Li, *et al.*, *New England Journal of Medicine* **382**, 1199 (2020). PMID: 31995857.
[12] J. Zhang, *et al.*, *The Lancet Infectious Diseases* **20**, 793 (2020).
[13] RIVM, Beschrijving transmissiemodel berekening zorgbelasting, https://www.rivm.nl/documenten/beschrijving-transmissiemodel-berekening-zorgbelasting (2021). Online; accessed 30 March 2022.
[14] A. J. Kucharski, *et al.*, *The Lancet Infectious Diseases* **20**, 1151 (2020).
[15] W. H. Press, R. C. Levin, *Science* **370**, 1015 (2020).
[16] M. Cevik, S. D. Baral, *Science* **373**, 162 (2021).
[17] J. A. Backer, *et al.*, *Eurosurveillance* **26** (2021).
[18] S. J. de Vlas, L. E. Coffeng, *Scientific Reports* **11**, 4445 (2021).
[19] M. Pavelka, *et al.*, *Science* **372**, 635 (2021).
[20] S. Mallapaty, *Nature* **580**, 176 (2020).
[21] E. C. Lee, N. I. Wada, M. K. Grabowski, E. S. Gurley, J. Lessler, *Science* **370**, 406 (2020).
[22] J. D. Munday, *et al.*, *Nature Communications* **12**, 1942 (2021).
[23] J. Lessler, *et al.*, *Science* **372**, 1092 (2021).
[24] M. C. Castro, *et al.*, *Science* **372**, 821 (2021).
[25] W. M. de Souza, *et al.*, *Nature Human Behaviour* **4**, 856 (2020).
[26] R. Laxminarayan, *et al.*, *Science* **370**, 691 (2020).
[27] D. A. Drew, *et al.*, *Science* **368**, 1362 (2020).
[28] N. Oliver, *et al.*, *Science Advances* **6**, eabc0764 (2020).
[29] L. Ferretti, *et al.*, *Science* **368**, eabb6936 (2020).
[30] B. J. Quilty, *et al.*, *BMC Medicine* **18**, 259 (2020).
[31] L. C. Herng, *et al.*, *Scientific Reports* **12**, 2197 (2022).
[32] S. Moritz, *et al.*, *Nature Communications* **12**, 5096 (2021).
[33] J. E. Lemieux, *et al.*, *Science* **371**, eabe3261 (2021).
[34] Google, Google Community Mobility Report 2020, https://www.google.com/covid19/mobility/ (2021). Online; accessed 31 October 2021.

Acknowledgments

The authors thank Mirjam Kretzschmar for a careful reading of the manuscript.
Funding: The authors gratefully acknowledge financial support via ZonMw grant 10430022010001. In addition, LEC acknowledges funding from the Dutch Research Council (NWO, grant 016.Veni.178.023).
Author contributions: All authors contributed to the research conceptualization. MMD and LEC, with help of all authors, conceived the framework principles. MMD performed the analysis. All authors contributed to writing.
Competing interests: The authors declare no competing interest.
Data and materials availability: Data associated with mobility and mixing reductions (Google mobility and PIENTER) is publicly available [17, 34]. Age-stratified mixing matrices used in the analysis (POLYMOD) are publicly available as described in [9]. Hospital admission data (NICE) is publicly available as described in SI A.5. Our analysis also uses mobility information from Mezuro as input. This data is owned by a commercial party and can therefore not be made public. Analysis codes will be made available upon publication.

Supplementary Materials

SI A - Analysis framework components
SI B - Additional model results